Supplemental Material

Influence of interfaces on the phonon density of states of nanoscale metallic multilayers:

Phonon confinement and localization

W. Keune[1], Sampyo Hong[2,3], M. Y. Hu[4], J. Zhao[4], T. S. Toellner[4], E. E. Alp[4], W. Sturhahn[5], T. S. Rahman[2#], B. Roldan Cuenya[2,6*]

[1]*Department of Physics, University of Duisburg-Essen, 47057 Duisburg, Germany*

[2]*Department of Physics, University of Central Florida, Orlando, FL 32816, USA*

[3]*Division of Physical Sciences, Brewton-Parker College, Mount Vernon, GA 30445, USA*

[4]*Advanced Photon Source, Argonne National Laboratory, Lemont, IL 60439, USA*

[5]*Seismological Laboratory, California Institute of Technology, Pasadena, CA 91125, USA*

[6]*Department of Interface Science, Fritz-Haber Institute of the Max Planck Society, 14195 Berlin, Germany*

E-mail: * roldan@fhi-berlin.mpg.de ; # talat@ucf.edu

I. Structural characterization

Crystallographic orientation

Figure S1 shows conventional high-angle (Θ - 2Θ) X-ray diffraction (XRD) patterns of the two Fe/Ag multilayers, i.e., of the interface and center Fe layer, respectively. Both scans are very similar, providing evidence for the good reproducibility of our sample preparation method. The strong peak near 2Θ ~ 44° (peak 1) and the weaker reflections near ~ 65° (peak 2) and ~ 98° (peak 3) can be assigned to the Ag(200)/Fe(110), Ag(220)/Fe(200) and Ag(400)/Fe(220) Bragg reflections [36]. It is known that the Fe(110), Fe(200) and Fe(220) reflections are severely overlapping with the Ag(200), Ag(220) and Ag(400) reflections, respectively, and can be hardly resolved [36]. However, as the atomic scattering factor (f^2) of Ag is significantly larger than that of Fe (e.g., by a factor of ~ 4.4 near 2Θ = 44° according to ref. [44]), the Fe peak intensities are much weaker than those of the overlapping stronger Ag reflections. In our case, the intensity ratio of peak 1 to peak 2 is 8.2 and 7.8 for the

interface sample and the center sample, respectively. (In Ag powder samples this intensity ratio is found to be only 1.7). Also, one can notice that the Ag(111) reflection is absent in Fig. S1. These observations provide evidence of a pronounced crystallographic (200) texture of the Ag layers in both samples, in agreement with Ref. [36]. Our XRD data in Fig. S1 do not allow to draw direct conclusions on the textured growth of the Fe layers in our Fe/Ag multilayers. However, in case of a very strong Ag(002) texture, which appears to be the case here, one can assign peak 2 near ≈ 65° in Fig. S1 to the Fe(200) reflection (which is then dominant over the Ag(220) reflection, the latter being suppressed due to the Ag(002) texture). Therefore, there is justification to assume that our thin Fe layers (13.5 Å), deposited at 180 °C, preferably grow with (200)-texture on the (200)-textured Ag films throughout the complete multilayers. This type of orientation is favorable, since the two (200) surface nets of bcc Fe and fcc Ag are in almost perfect in-plane registry after a mutual rotation of 45° about the surface normal [40], and Fe(200)/Ag(200) epitaxial growth (which often is labeled as Fe(001)/Ag(001) epitaxy in surface physics) often has been observed in the literature [41-43].

Assuming that peak 1 (near ≈ 44°) and peak 3 (near ≈ 98°) in Fig. S1 solely originate from Ag(200) and Ag(400) and peak 2 (near ≈ 65°) predominantly from Fe(200) reflections, then the XRD scans in Fig. S1 provide the following (out-of-plane) lattice parameters for Ag and Fe, respectively: a_{Ag} = 4.061 Å, a_{Fe} = 2.892 Å for the interface sample, and a_{Ag} = 4.071 Å, a_{Fe} = 2.884 Å for the center sample. The lattice parameter of the Ag (Fe) layers in our multilayers is slightly reduced (enhanced) with respect to the value of the bulk material (a_{Ag}(bulk) = 4.086 Å and a_{Fe}(bulk) = 2.866 Å) [43]. Considering the assumed Fe(200)/Ag(200) [equivalent to Fe(001)/Ag(001)] textured growth of our multilayers, the individual layer thicknesses of t_{Fe} = 13.5 Å and t_{Ag} = 16 Å can be expressed in units of monolayers (ML) as t_{Fe} = 9.4 ML (= 8 ML of ^{56}Fe + 2 x 0.7 ML of ^{57}Fe) and t_{Ag} = 8 ML, respectively. Similar layer thicknesses of 8 ML for Fe and 8 ML of Ag were considered in our theoretical calculations.

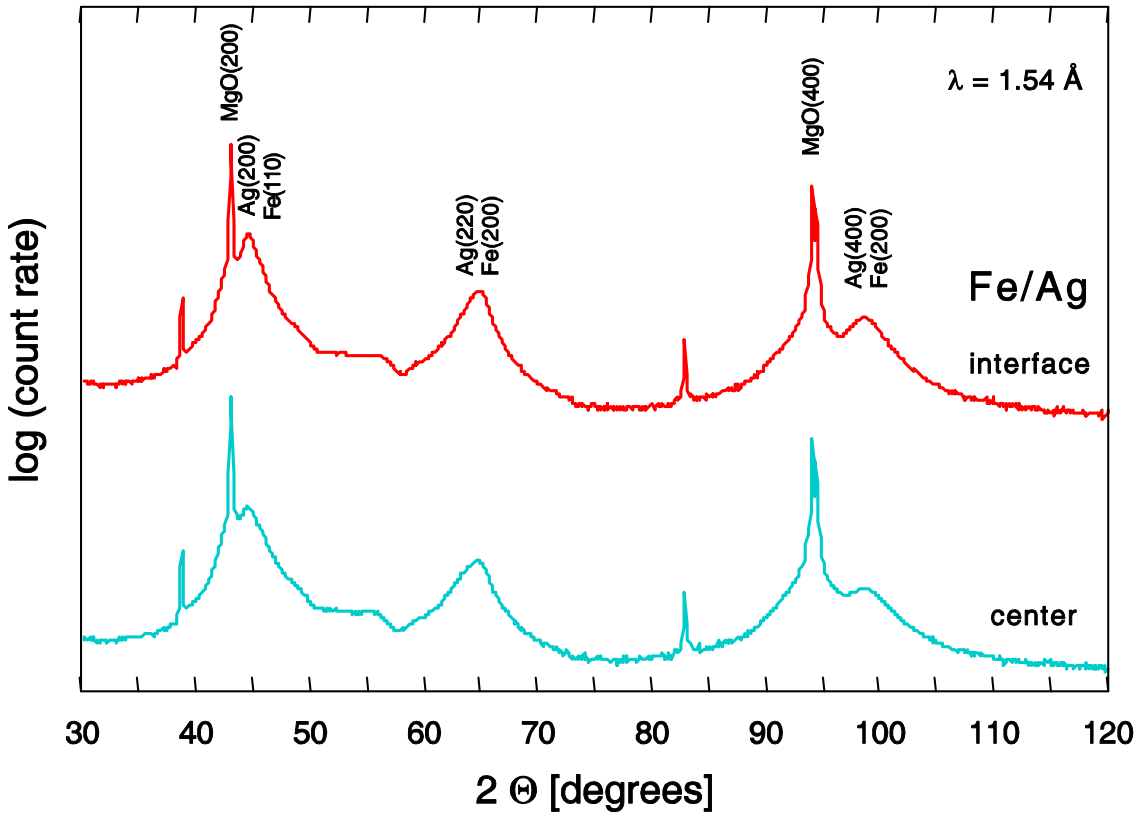

FIG. S1*:* (Color online) *X-ray diffraction (Θ - 2Θ) patterns of Fe/Ag multilayers. Top: "interface" sample* $[Ag(8ML)/^{57}Fe(0.7ML))/^{56}Fe(8ML)/^{57}Fe(0.7ML)]_{100}$*. Bottom: "center" sample* $[Ag(8ML)/^{56}Fe(4ML)/^{57}Fe(1.4ML)/^{56}Fe(4ML)]_{57}$*. (Cu-*$K_\alpha$ *radiation,* $\lambda = 1.54$ *Å). The Ag(200)/Fe(110) (peak 1), Ag(220)/ Fe(200) (peak 2) and Ag(400)/Fe(220) (peak 3) reflections are indexed. (Please notice the logarithmic vertical scale).*

Multilayer Periodicity

Fig. S2 displays the small-angle (Θ - 2Θ) X-ray reflectivity patterns of the multilayers $[Ag(8ML)/^{57}Fe(0.7ML)/^{56}Fe(8ML)/^{57}Fe(0.7ML)]_{100}$ (interface sample) and $[Ag(8ML)/^{56}Fe(4ML)/^{57}Fe(1.4ML)/^{56}Fe(4ML)]_{57}$ (center sample), together with a simulation for the ideal [Ag(8ML)/Fe(9.4ML)] multilayer system with homogeneous layers and sharp interfaces. Both samples show only a weak first-order superlattice reflection at $2\Theta \approx 3°$, and no higher-order interferences. The position of the simulated first-order peak approximately coincides with the corresponding position of the measured first-order reflection of both samples. This proves that in average the nominal Fe-Ag bilayer period agrees with the measured bilayer period. However, the absence of measured higher-order reflections demonstrates large interface roughness in our multilayers at such low individual film thicknesses of t_{Fe} = 13.5 Å (9.4 ML) and t_{Ag} = 16 Å (8 ML). We conclude that the individual Fe and Ag films are no homogeneous films, but have an island structure, as in

similar Fe/Ag multilayers described in the literature [36]. However, we may exclude severe chemical intermixing of Fe and Ag as a reason for the disappearance of higher-order reflections in Fig. S2, as demonstrated by our ^{57}Fe conversion-electron Mössbauer spectra (CEMS) on these samples (see Fig. 2(a),(b) in the main text).

The X-ray θ-2θ specular scans shown in Fig. S2 provide only a qualitative picture of the Fe/Ag interface roughness. In order to obtain quantitative information on the presumed interfacial island structure, one has to measure and to model the off-specular diffuse X-ray intensity [45]. However, this is beyond the scope of the present work.

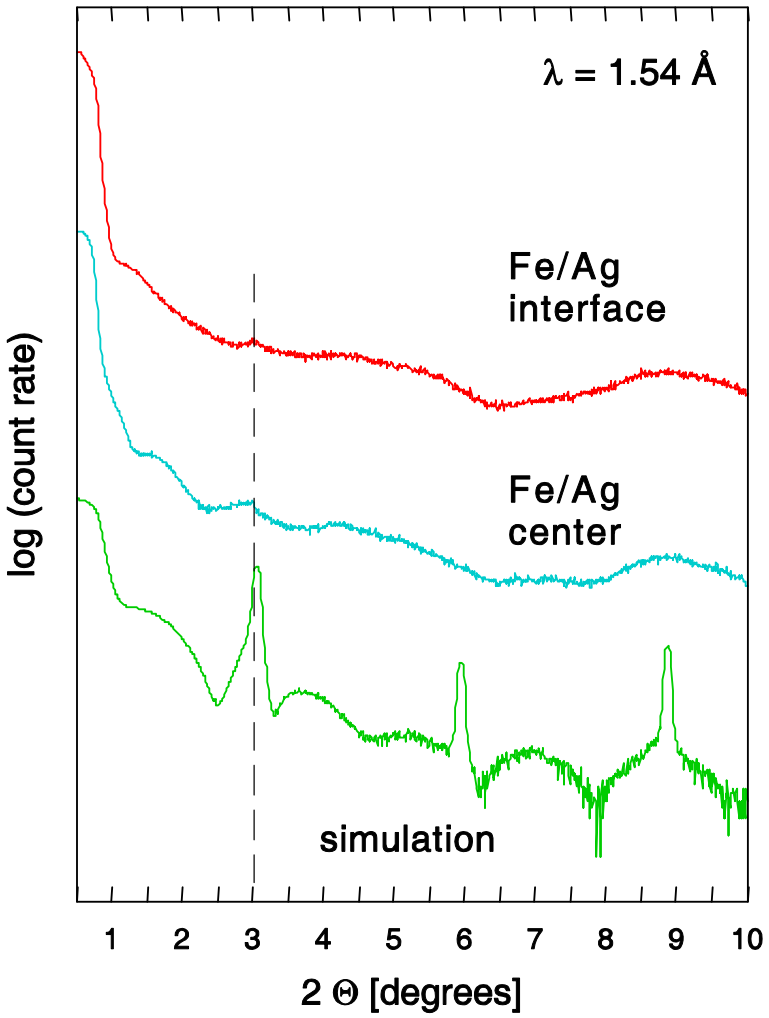

FIG. S2: (Color online) *Small-angle X-ray reflectivity patterns of Fe/Ag multilayers .(Cu-K_α radiation, λ= 1.54 Å). Top: "Interface" sample [Ag(8ML)/$^{\delta 7}$Fe(0.7ML)/$^{\delta 6}$Fe(8ML)/$^{\delta 7}$Fe(0.7ML)]$_{100}$. Middle: "center" sample [Ag(8ML)/$^{\delta 6}$Fe(4ML)/$^{\delta 7}$Fe(1.4ML)/$^{\delta 6}$Fe(4ML)]$_{57}$. Bottom: Simulation for [Ag(8ML)/Fe(9.4ML)] multilayer with ideally layered structure and ideally sharp interfaces. The vertical dashed line indicates the position of the first-order superlattice reflection. (Please notice the logarithmic vertical scale).*

The following Table SI shows Mössbauer parameters obtained by least-squares fitting the Mössbauer spectra in Figure 2 (main text).

Table SI: Mössbauer parameters of the Fe/Ag and Fe/Cr multilayers at room temperature, obtained by least-squares fitting the CEM spectra in Fig. 2 (a) and (b) of the main text, respectively. $<B_{hf}>$ = (average) hyperfine field, $<\delta>$ = (average) isomer shift (relative to α-Fe at room temperature), $x = I_2/I_3 = I_5/I_4$ = sextet line intensity ratio, $<\Theta>$ = average Fe spin canting angle (relative to the film surface normal), A = relative intensity (spectral area) of the fitted subspectrum. The numbers in brackets indicate the statistical error margins. Numbers with a * were kept fixed during the least-squares fitting.

Sample/(sample code)		**$<B_{hf}>$ (T)**	**$<\delta>$ (mm/s)**	**x**	**$<\Theta>$ (□)**	**A (%)**
Fe/Ag interface (AG10)	distribution $P(B_{hf})$	30.1(1)	0.169(2)	3.6*	77*	26(7)
	sharp sextet	32.9(1)	0.036(1)	3.6(1)	77(6)	74(7)
Fe/Ag center (AG11)	sharp sextet	32.3(1)	0.016(1)	3.5(1)	75(5)	100.0
Fe/Cr interface (arg03a)	distribution $P(B_{hf})$	22.2(1)	-0.085(1)	3.6(1)	77(1)	79(6)
	sharp sextet	33.3(1)	0.006(1)	4.0*	90*	21(6)
Fe/Cr center (arg04a)	distribution $P(B_{hf})$	29.1(3)	-0.01(2)	3.0(1)	68(2)	41(7)
	sharp sextet	33.1(1)	0.01(1)	3.0(1)	68(2)	59(7)

II. Nuclear resonance inelastic X-ray scattering (NRIXS) spectra of Fe/Ag and Fe/Cr multilayers

Figures S3 and S4 exhibit the NRIXS spectra (raw data) of the two Fe/Ag and of the two Fe/Cr multilayer samples, respectively, measured at room temperature at beamline 3-ID of the Advanced Photon Source at the Argonne National Laboratory (USA). Positive energy transfer refers to phonon creation, while negative energy transfer refers to phonon annihilation. The strong central zero-phonon (elastic) peak (or Mössbauer line) at zero energy transfer has been cut for clarity.

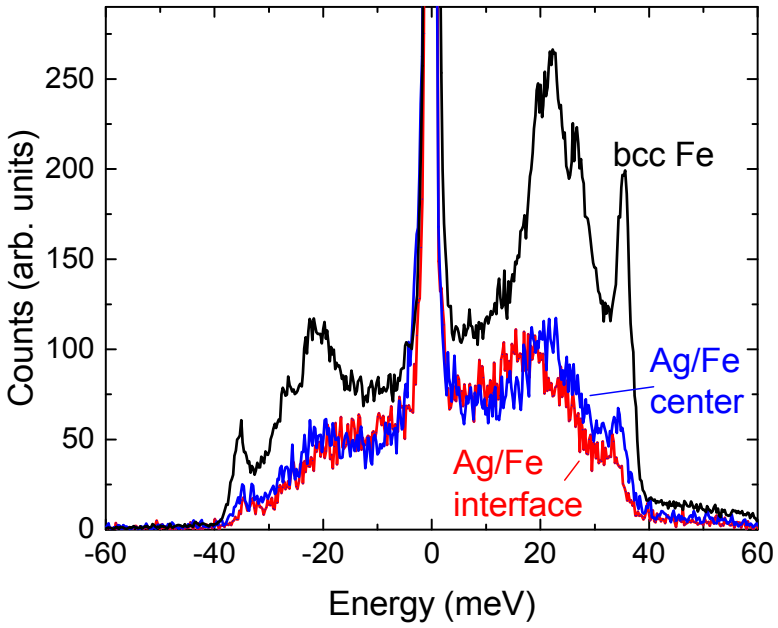

FIG. S3: (Color online) *^{57}Fe NRIXS spectra measured at room temperature on Fe/Ag multilayers. All samples contain ^{57}Fe probe layers. Red line: [Ag(8ML)/$^{\delta 7}$Fe(0.7ML)/$^{\delta 6}$Fe(8ML)/$^{\delta 7}$Fe(0.7ML)]$_{100}$ (interface sample); Blue line: [Ag(8ML)/$^{\delta 6}$Fe(4ML)/$^{\delta 7}$Fe(1.4ML)/$^{\delta 6}$Fe(4ML)]$_{57}$ (center sample). For comparison, also the spectrum of bulk bcc Fe at room temperature is shown (black line). The energy resolution ΔE is 0.9 meV. The huge central elastic peak at energy transfer E = 0 meV was cut off for clarity. The vertical scale is a linear scale.*

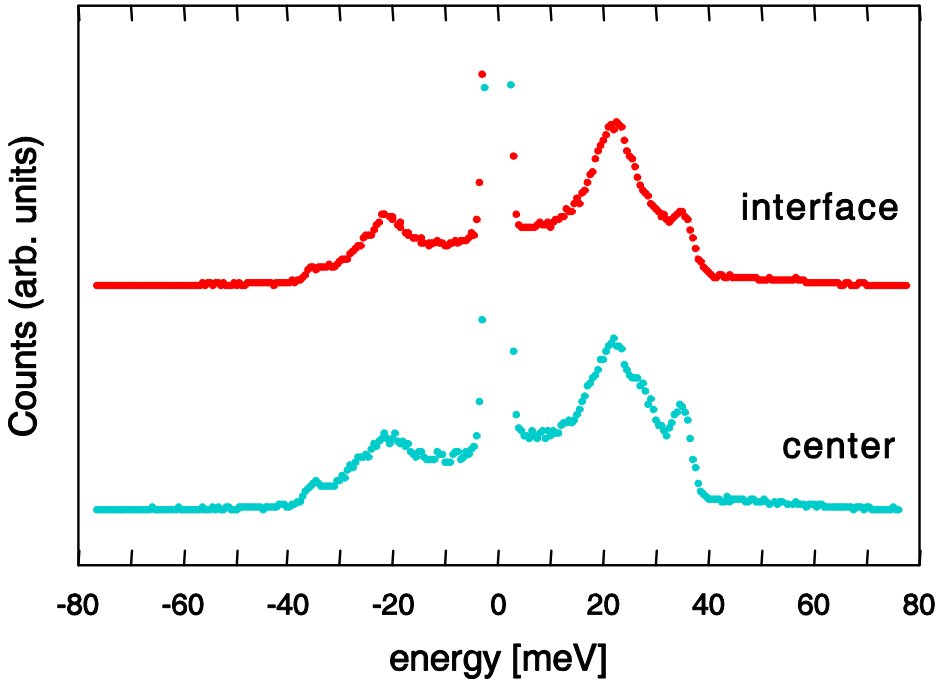

FIG. S4: (Color online) *^{57}Fe NRIXS spectra measured at room temperature on Fe/Cr multilayers. All samples contain ^{57}Fe probe layers. Red dots: [Cr(8ML)/^{57}Fe(0.7ML)/^{56}Fe(8ML)]$_{200}$ (interface sample). Blue dots: [Cr(8ML)/^{56}Fe(4ML)/^{57}Fe(0.7ML)/^{56}Fe(4ML)]$_{200}$ (center sample). The energy resolution ΔE is 2.3 meV. The huge central elastic peak at energy transfer E = 0 meV was cut off for clarity. The vertical scale is a linear scale.*

III. Phonon Dispersion Curves of Fe/Ag and Fe/Cr multilayers

As discussed in the manuscript, the Fe/Ag system has a high electron spin polarization (79 %) at the Fermi energy. Furthermore, the occurrence of large charge transfer at the interface (0.15 electrons for Fe/Ag and 0.32 electrons for Fe/Cr) can make the Fe/Ag and particularly Fe/Cr multilayers electrostatically unstable. Our calculated phonon dispersion curves of the Fe/Ag and Fe/Cr multilayers in Figures S5 and S6, respectively, strongly indicate such instability. In Figure S5 the Fe/Ag system exhibits a negative mode at/around the Γ point indicating a long-ranged instability involving the ideally-flat Fe/Ag interface. More interesting is the Fe/Cr system, which exhibits much more pronounced negative modes at/around the Γ point (and also at the X point) in Fig. S6. In fact, this is not surprising considering that in the ideally-flat Fe/Cr interface much larger charge transfer, more than twice than that of the Fe/Ag interface, occurs. (Vibrations involving the Fe/Cr interface can cause significant change in Fe-Cr bond length, which could induce substantial variation in charge transfer and thereby similar ones in energy and force leading to substantial softening in the force constants.) In Figure S6 we observe several softening modes along the Γ-Z and Γ-X directions.

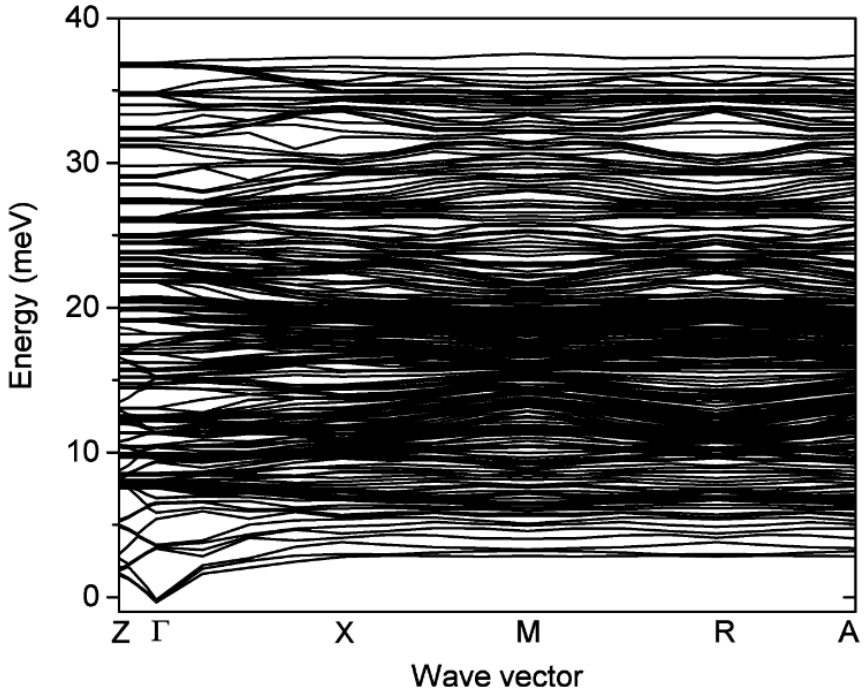

FIG. S5: *Calculated phonon dispersion curves of the Fe/Ag multilayer with the ideally flat Fe/Ag interface along the high symmetric points Z-Γ-X-M-R-A.*

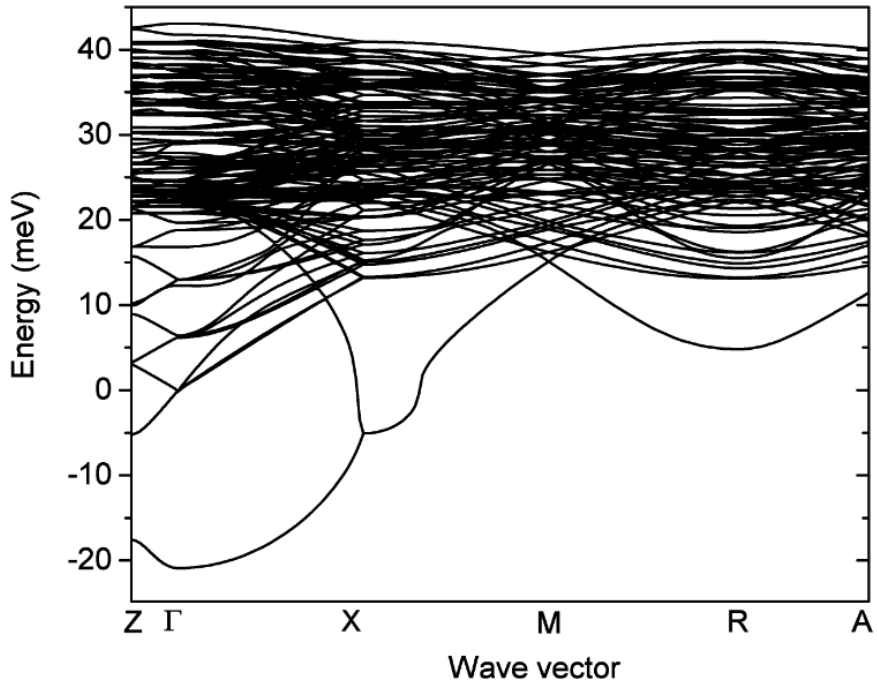

FIG. S6: *Calculated phonon dispersion curves of the Fe/Cr multilayer with the ideally flat Fe/Cr interface along the high symmetric points Z-Γ-X-M-R-A.*

IV. Comparison of theoretical unprojected, theoretical direction-projected and experimental Fe-VDOS for Fe/Cr multilayers

In the figure below a comparison is made among the calculated unprojected (total) partial Fe-VDOS, the calculated direction-projected partial Fe-VDOS and the experimental partial Fe-VDOS for the Fe/Cr multilayers.

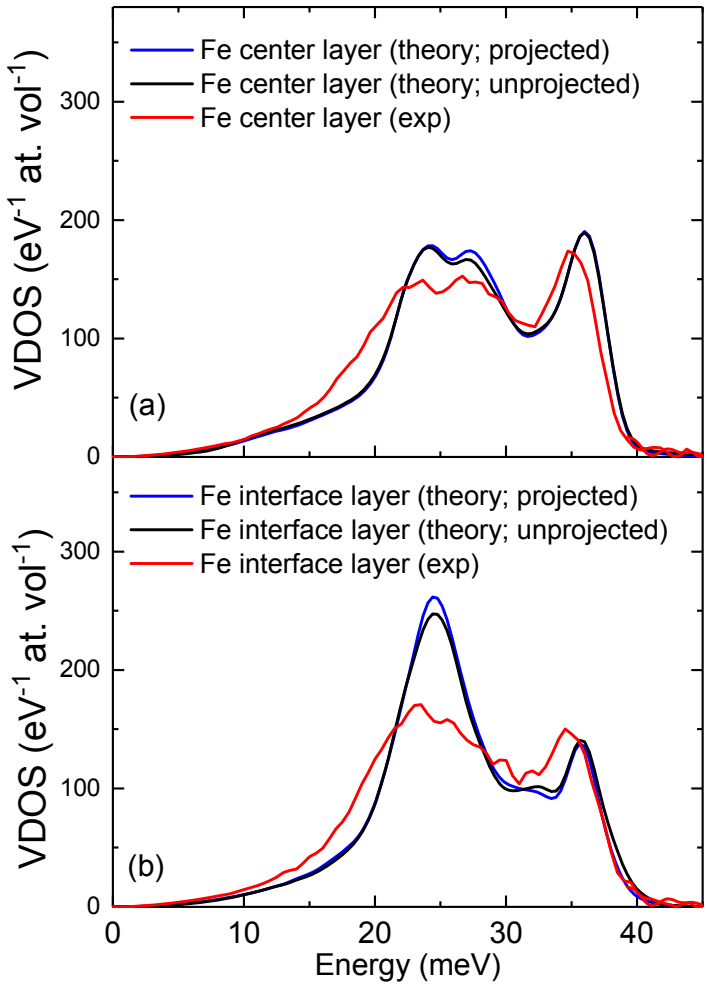

FIG. S7: (Color online) *A comparison among unprojected (from Fig. 4(b)) and direction-projected theoretical Fe-VDOS and experimental Fe-VDOS (from Fig. 3(b) for Fe/Cr(001) multilayers. The areas below the theoretical VDOS curves are normalized according to the experimental VDOS.* ***(a)*** *The theoretical unprojected (black line) and direction-projected (blue line) Fe-VDOS of Fe/Cr at the center together with the experimental (red line) VDOS for the Fe/Cr center layer);* ***(b)*** *The theoretical unprojected (black line) and direction-projected (blue line) Fe-VDOS of Fe/Cr at the interface together with the experimental (red line) VDOS for the Fe/Cr interface).*

References (for supplemental material, SM):

(The reference numbers for the SM in the list below correspond to the reference numbers in the list of references of the main text).

[36] Y. Kozono, M. Komura, S. Narishige, M. Hanazono, and Y. Sugita, J. Appl. Phys. **63**, 3470 (1988).

[40] B. T. Jonker and G. A. Prinz, Surf. Sci. **172**, L568 (1986).

[41] N. C. Koon, B. T. Jonker, F. A. Volkening, J. J. Krebs, and G. A. Prinz, Phys. Rev. Lett. **59**, 2463 (1987).

[42] M. Stampanoni, A. Vaterlaus, M. Aeschlimann, and F. Meier, Phys. Rev. Lett. **59**, 2483 (1987).

[43] D. E. Bürgler, C. M. Schmidt, D. M. Schaller, F. Meisinger, R. Hofer, and H.-J. Güntherodt, Phys. Rev. B **56**, 4149 (1997).

[44] B. E. Warren, *X-Ray Diffraction* (Addison-Wesley, Reading, Mass., 1989) pp. 370-371.

[45] A. Schreyer, J. F. Ankner, Th. Zeidler, H. Zabel, M. Schäfer, J. A. Wolf, P. Grünberg, and C. F. Majkrzak, Phys. Rev. B **52**, 16066 (1995).